Research Square

Preprints are preliminary reports that have not undergone peer review.
They should not be considered conclusive, used to inform clinical practice,
or referenced by the media as validated information.

New fossil records of Megantereon (Carnivora: Machairodontinae) from Northwestern China

Dingge Guo
Institute of Vertebrate Paleontology and Paleoanthropology
Joan Madurell Malapeira
Università Di Firenze
Dmitriy O Gimranov
Russian Academy of Sciences
Luda Xing
Institute of Vertebrate Paleontology and Paleoanthropology
Peiran Li
Institute of Vertebrate Paleontology and Paleoanthropology
Dongting Huang
Institute of Vertebrate Paleontology and Paleoanthropology
Haiyan Ma
Hezheng Paleozoological Museum
Yi Jia
Hezheng Paleozoological Museum
Lu Zhang
Hezheng Paleozoological Museum
Qigao Jiangzuo
jiangzuo@ivpp.ac.cn

Institute of Vertebrate Paleontology and Paleoanthropology
Shiqi Wang
Institute of Vertebrate Paleontology and Paleoanthropology

Research Article

Keywords: ecotone, Longdan, M. microta, Paleoecology, Quaternary

Posted Date: September 25th, 2026

DOI: https://doi.org/10.21203/rs.3.rs-10998694/v1

License: This work is licensed under a Creative Commons Attribution 4.0 International License. Read Full License

Additional Declarations: No competing interests reported.

Abstract

Northwestern China has yielded abundant *Megantereon* fossils in the early Pleistocene, with the most representative being *M. nihowanensis*. By the late Early Pleistocene, this lineage further evolved into a larger sized form with more derived dentition, *M. inexpectatus*. This study reports the identification of a third form of *Megantereon* from Shitougou, the classical Earliest Pleistocene locality of the Longdan Fauna in Gansu Province. This form, here assigned to *M. microta*, is represented by a complete mandible. Compared with the much more abundant material of *M. nihowanensis* of the same locality, it is significantly smaller in size and show clear different morphology, specifically with very short c-p3 diastema, larger mental flange, and larger and double rooted p3. It is similar in size and dental morphology to southern Chinese *M. microta*, but possesses a more robust mandible and more strongly developed lower incisors and canines, though these differences remain within intraspecific variation. Furthermore, the Longdan fauna includes several typical Oriental species, indicating that although the region exhibited a relatively dry and cold overall environment during the Early Pleistocene, relatively humid local habitats likely still existed. This faunal composition indicates that the area represented an ecotone (a transition zone between two ecosystems) between northern and southern faunal provinces. This interpretation provides new key evidence for deeply understanding the pattern of the paleoecological environment in the Longdan region during the Early Pleistocene, as well as the dynamics of migration and interchange between the northern and southern faunas during this period.

Introduction

The Linxia Basin contains an abundance of relatively complete and densely clustered large mammal fossils, spanning from the Late Oligocene to the Late Pleistocene (based on new, unpublished fossil records), undergoing a succession of faunal changes (Deng et al. 2023; Wang et al. 2023). Within this basin, the Longdan area is particularly notable for yielding abundant fossils with abundant *Equus* remains, dated to 2.2–2.5 Ma, often referred to as the Early Pleistocene *Equus* Fauna (Longdan Fauna). Additionally, this fauna exhibits remarkably high carnivore diversity (Deng 2004; Qiu et al. 2004; Jiangzuo et al. 2023). The Felidae reached their peak abundance during this period, with *Megantereon nihowanensis* emerging as a particularly dominant among the large felids (Qiu et al. 2004; Jiangzuo et al. 2023). In addition to *Megantereon*, the felids of the Longdan Fauna include *Homotherium crenatidens*, *Acinonyx linxiaensis*, *Panthera palaeosinensis*, *Lynx issiodorensis*, and *Lynx hei* (Qiu et al. 2004; Jiangzuo et al. 2022; Jiangzuo et al. 2023).

The Longdan area preserves a large number of *Megantereon* fossils. All previously discovered materials from this area have been assigned to *M. nihowanensis*, and this species that is relatively widespread in East Asia, particularly in China (Qiu et al. 2004; Zhu et al. 2020). In the Longdan area, *Megantereon* exhibits certain intraspecific variability, such as differences in body size: individuals from the lower layers are smaller, while those from the upper layers are larger (Qiu et al. 2004). Additionally, morphological variance is also present in the cranium and teeth (Guo et al. 2025). The measurements of the holotype specimen from Nihewan fall within the range of variation observed in the Longdan specimens (Qiu et al. 2004). During this period, certain specimens of *M. nihowanensis* from the Longdan area already exhibit incipient morphological features transitional toward *M. inexpectatus*, such as an angled frontal convexity, elongated P3 and P4, and a reduced protocone on P4 (Guo et al. 2025).

All previously reported specimens of *Megantereon microta* are from southern China (in Fig. 1), but the holotype from Yanliang Cave, Chongzuo, Guangxi is the only relatively complete mandible, whereas all other materials, including those from Longgudong in Jianshi, Hubei, the Gigantopithecus Cave in Liucheng, Guangxi, and the Yuanmou area in Yunnan, consist solely of isolated teeth (You et al. 1978; Pei 1987; Zhang and Feng 2004; Zhu et al. 2014; Zhu et al. 2020). This study will conduct a detailed comparative analysis of a unique mandible from the Longdan region. Notably, this specimen does not belong to the locally common *M. nihowanensis*, but instead shows closer affinities to the smaller-sized *M. microta*, which is previously only known in southern China. This finding suggests that Longdan was an ecotone during the Early Pleistocene, a transitional zone where northern and southern faunal communities overlapped, and such a zone would have promoted the convergence of distinct lineages

Geological background

Fossils of the Longdan Fauna are found at Longdan and three other nearby localities: Keshijian and Shitougou in Nalesi Township, and Xijia in Zhaojia Township, Guanghe County. Their lithology is very similar, as they are all directly deposited on top of the Jishi Formation conglomerate and overlain by the Malan Loess (Qiu et al. 2004). Situated in a small fault basin at the transition zone between the northeastern Qinghai-Tibet Plateau and the Loess Plateau, the Longdan area endows its fauna with typical Loess Plateau biological elements as well as some remnants of the Qinghai-Tibet and East Indian faunas (Xue et al. 2006). Mammalian fossils in the Longdan section are mainly yielded from two horizons in the middle of the Wucheng Loess.

The fossil materials were collected from the Wucheng Loess at the Shitougou site (35°31'11.3"N, 103°29'19.7"E), in Nalesi Town, Dongxiang County, Gansu Province, China. Located 600 meters south of Longdan, the Shitougou section exhibits lithology and stratigraphic sequence highly consistent with those of the Longdan section, with only minor differences. Calcareous nodules are extremely well-developed in the loess of the Shitougou section. Due to the poor exposure conditions of the Longdan fauna section, there have long been different opinions regarding the precise age and paleoenvironmental background of the Longdan fauna (Zan et al. 2016). Deng (2002) reported that the lowermost part of the Longdan section in the Linxia Basin coincides with the Matuyama-Gauss boundary (Fang et al. 1997), and thus estimated the age of the Longdan Fauna to be ~ 2.5 Ma. Qiu et al. (2004) estimated the section at 2.58–2.15 Ma based on the Wucheng Loess, with the lower and upper fossil layers at ~ 2.55 Ma (below Réunion) and ~ 2.16 Ma (above Matuyama-Gauss), respectively, and assigned the fauna an age of ~ 2.2 Ma on the basis of mammalian evolutionary stage. Liu et al. (2008) revised the upper layer to ~ 1.9 Ma (Olduvai) and the lower to ~ 2.25 Ma (below Réunion), but their section was compromised by Malan Loess cover, fluvial reworking, and ambiguous GPTS correlation (Hilgen et al. 2012; Zan et al. 2016). Zan et al. (2016) obtained 2.2 Ma (upper) and 2.5 Ma (lower) from a 105-m core. Liu et al. (2023) applied cosmogenic $^{26}Al/^{10}Be$ and $^{10}Be/^{21}Ne$ burial dating and proposed a younger age of 2.1–1.9 Ma, circumventing the stratigraphic limitations of magnetostratigraphy.

Some scholars consider that the Longdan Fauna represents a more primitive evolutionary grade compared with other Quaternary faunas in northern China, particularly the Nihewan Fauna, even at the congeneric level (Qiu et al. 2004; Deng et al. 2013). This is manifested in the presence of certain primitive forms in the Longdan Fauna that are absent in the Nihewan Fauna, such as *Leptobos brevicornis*, *Metacervocerus longdanensis*, *Canis teilhardi* and *Crocuta honanensis* (Qiu et al. 2004; Shi 2023). Conversely, the Nihewan Fauna possesses some advanced forms not found in the Longdan Fauna, such as *Bison palaeosinensis* and *Metacervocerus elegans* (Qiu et al. 2004; Deng et al. 2013; Shi 2023). The Xiashagou Fauna, i.e., the Nihewan Fauna sensu stricto, was long considered close in morphology and evolutionary level to the Olivola Fauna of the European Villafranchian, with an age of approximately 1.8 Ma (Qiu 2000). However, according to Farjand et al. (2023), the classic Nihewan Fauna should be constrained to 2.4–1.8 Ma, based on the correlation of fossil horizons with the magnetostratigraphy of the Xiashagou section (Liu et al. 2012; Liu et al. 2016) and linear interpolation. From the perspective of mammalian evolutionary stage, the age model of 2.5–2.2 Ma for the Longdan Fauna is more consistent with its fauna being slightly older than the Nihewan Fauna, and thus represents a more reliable chronological framework.

Materials and methods

The *Megantereon* material described here is housed in the Institute of Vertebrate Paleontology and Paleoanthropology, Chinese Academy of Sciences. For comparison, *Megantereon* specimens from HMV, IVPP, THP were checked for comparison.

The data of *Panthera tigris* and *Panthera pardus* from IOZ and IVPP were also used.

The location and chronology of fossil localities are illustrated in Fig. 1.

For the craniodental measurements see Jiangzuo and Liu (2020) and Fig. 2. The terminology of cranium follows Qiu et al. (2014) with modification.

To restore the anterior compression deformation in the new Longdan material caused by external forces, we 3D scanned the specimen using an Artec Spider scanner. We then used Artec Studio 14 Professional to reconstruct the pre-deformation morphology and measured the data. These restored data were used in the subsequent box plots and PCA analysis.

We used PAST 4.04 to perform box plot analysis on the c-p3 diastema / p3-m1 ratio of *Megantereon* mandibles, and to conduct principal component analysis (PCA) on *Megantereon* and extant *Panthera*.

H4 represents the maximum vertical height from the apex of the coronoid process to the base of the angular process. **W4** represents the maximum mediolateral transverse width of the condylar process

Anatomical abbreviations

H

Height

L

Mesiodistal length

M/m

Upper/lower molar

P/p

Upper/lower premolar

W

Buccolingual width

Repositories and institutional abbreviations: CECC, Center for Conservation and Etude of Collections, Lyon, France; HMV, Hezheng Paleozoological Museum; IOZ, Institute of Zoology, Chinese Academy of Sciences; IVPP, Institute of Vertebrate Paleontology and Paleoanthropology, Chinese Academy of Sciences; MNHN, National Museum of Natural History, Paris, France; THP, Tianjin Natural History Museum

Systematic palaeontology

Family Felidae Batsch, 1788

Subfamily Machairodontinae Gill, 1872

Tribe Smilodontini Kretzoi, 1929

Genus *Megantereon* Croizet et Jobert, 1828

Megantereon microta Zhu et al. 2014

Holotype

IVPP V19015.1. A complete mandible lacking the p3, from Yanliang Cave, Chongzuo.

Described material: IVPP V34763, a complete right mandible.

Emended diagnosis

Small sized *Megantereon*, size similar to or slightly exceeding that of primitive *Megantereon megantereon*, mandibular symphysis verticalized and mandibular flange relatively well-developed, p3 double-rooted, short c-p3 diastema, moderately developed coronoid process.

Description (Fig. 3)

Body size is relatively small. The mandible is relatively short, wide, and robust, with notable thickness in the mandibular corpus below the buccal tooth row. The mandibular flange is well-developed, extending anteriorly and distinctly ventrally. In anterior view, the symphysis is narrow superiorly and broad inferiorly. The upper part of the symphysis (rostral portion) curves slightly forward, whereas the middle-lower part is somewhat concave. The ventral margin of the symphysis exhibits a distinct upward-convex inverted U-shape. The mental crest extends distally, with an irregular and undulating margin. Viewed from the lateral side, the area at the c-p3 diastema is compressed and forms a distinct inward triangular depression with cracks. A small foramen, presumably the mental foramen, is visible in this fractured area. From the anterior margin of p3, the ventrolateral margin of the diastema extends inward and upward at a low angle, then turns to extend outward and upward at a high angle to the posterior margin of the lower canine. Below this inflection point, on the lateral surface of the mandibular corpus, there is an oblique, elongated-oval mental foramen, positioned posteriorly and slightly superior to the other foramen. Anteroventral to the triangular depression, extending toward the mental protuberance, there is a distinct concavity that connects with the upper sub-triangular depression to form a receptacle for the upper canine. The ventral margin of the mandibular corpus is slightly convex downward at the mid-section and weakly constricted upward below the coronoid process. The masseteric fossa is deep, with its anterior margin slightly extending past the posterior margin of the lower cheek teeth. The coronoid process slopes posteriorly overall, with its distal tip broken. The condylar process is positioned relatively low, approximately at the mid-level of the mandibular corpus. In dorsal view, the anterior margin of the coronoid process slopes anteroventrally, developing a blunt crest that extends onto the ventromedial surface of the mandibular corpus. The medial side of the condylar process is slightly broken.

The i1 is broken. The apices of i2 and i3 curve posteriorly, with a ridge extending from the tip toward the lingual base of the crown on both the mesial and distal sides. An accessory cusp is present at the distolingual base of i2. The i3 is slightly larger than i2, but damage to its lateral side prevents confirmation of whether an accessory cusp is present. The lower canine is laterally convex and medially flat, possessing two ridges: one on the mesial side, and the other posterior to the c, which twists mesially as it extends from the tip toward the base. The posterior cheek teeth are closely packed without diastemata. The p3 is double-rooted and inclines posteriorly as a whole. Its lingual main cuspid and distal accessory cuspid are broken posteriorly, while the mesial accessory cuspid is reduced. A faint depression is visible anterior to the main cuspid, and the distal accessory cuspid forms a weakly protruding cusp. The p4 slopes posteriorly. Its mesial accessory cuspid connects anteriorly with the cingulum at the crown base, bulging forward, and is closely appressed to the main cuspid posteriorly. The distal accessory cuspid is nearly equal in size to the distal cingulid, which is pointed. The anterior and posterior blades of the m1 are separated by a carnassial notch, with the two blades being unequal in size, and the paraconid accounting for approximately one-third of the total length.

Measurements are given in Tables 1.

Table 1

Mandibular and lower dentition measurements of *Megantereon microta* from Longdan and Chongzuo. Values in parentheses indicate the specimen condition: **corr.**, corrected (virtually reconstructed) measurement; **orig.**, original (uncorrected) measurement. **H1-3**, mandibular height posterior to the canine (**H1**), anterior to p3 (**H2**), and posterior to m1 (**H3**); **W1-3**, corresponding mandibular widths; **H4**, maximum vertical height from the coronoid apex to the base of the angular process; **W4**, maximum mediolateral width of the condylar process

Mandible	**Locality**	**L1**	**c-m1**	**D c-p3**	**p3-m1**	**H1**	**W1**	**H2**	**W2**	**H3**	**W3**	**H4**	**W4**
IVPP V34763	Longdan	134.17 (orig.)	77.31 (orig.)	24.24 (orig.)	45.14	57.81	26.32	30.22	14.86	31.42	16.15	55.82+	37.61
		136.46 (corr.)	82.41 (corr.)	27.39 (corr.)									
IVPP V19015.1	Chongzuo	129.72	82.26	26.3	47.65	47.84	19.42	27.3	10.43	28.01	12.19	47.12	
Lower dentition		cL	cW	cH	p3L	p3W	p4L	p4W	m1L	m1PL	m1W		
IVPP V34763	Longdan	11.59	8.18	20.61	9.73	5.07	17.55	8.39	19.25	8.72	10.25		
IVPP V19015.1	Chongzuo	10.53	6.62	16.22			17.04	7.36	18.85	8.43	9.14		

Comparison

Compared with the most common sympatric species of Megantereon (M. nihowanensis/M. cultridens) (Fig. 4-d, e, f)

The new material differs markedly from *M. nihowanensis*, most notably in its significantly smaller body size, which is manifested in the mandible by a much shorter overall mandibular length. Although the upper portion of the mandibular symphysis in the new material (the alveolar base) is slightly anteriorly inclined, this inclination is far less pronounced than in *M. nihowanensis*, resulting in an overall vertical profile. Furthermore, the new material has a much shorter c-p3 diastema (in Fig. 6) and a somewhat more developed coronoid process relative to *M. nihowanensis*. Additionally, the cheek teeth of the new material exhibit several relatively primitive characteristics. For instance, p3 is double-rooted, and the ratio of p3 length to m1 length is relatively large, well exceeding the range of *M. nihowanensis*, indicating that p3 constitutes a larger proportion of the cheek tooth row. Conversely, the ratio of p4 length to m1 length falls within the range of *M. nihowanensis*.

Given that *M. cultridens* is the type species of *Megantereon*, and *M. nihowanensis* is widely considered conspecific with it by many authors due to the absence of characters exceeding interspecific variation, we will not reiterate the differences between the new Longdan material and *M. cultridens*. However, in this study we still treat *M. nihowanensis* as a distinct species and analyze it separately from *M. cultridens*.

Comparison with other small-sized Megantereon species

Megantereon megantereon is a very primitive species of *Megantereon*, with its type specimen originating from Perrier, France, dating to the Late Pliocene (~ 2.78 Ma) (Bravard 1828; Nomade et al. 2014). Specimen MNHN 1094 (Fig. 4-C) is a mandible of M. megantereon from Les Etouaires, Auvergne, France. It preserves a complete tooth row, although the mandibular flange, coronoid process, and the posterior portion

of the mandible are broken. As seen in specimen MNHN 1094, *M. megantereon* exhibits primitive characteristics in its mandible: a shorter c-p3 diastema (in Fig. 6), a very large proportional size of the premolars, a large, well developed p3 with a pointed mesial accessory cuspid, a distinct anterior cingulum, and a relatively short m1. The material from Kuruksay, Tajikistan, was assigned to a new subspecies, *Megantereon megantereon vakshhensis* (No. 1-694/H), dating to the Late Pliocene at approximately 2.6 Ma (Scharapov 1986, 1996). The anterior portion of this mandible is completely preserved, revealing a vertical mandibular symphysis. Compared to the material from Les Etouaires, the p3 in the Kuruksay material shows some reduction, including a shortened crown, reduced mesial accessory cuspid and anterior cingulum, and a lengthened p3-p4 diastema. It is worth noting, however, that the p4 of the Kuruksay material possesses a distinct mesial cingulid with a pointed tip, whereas no trace of a p4 mesial cingulid can be observed in the *M. megantereon* material. Compared with Les Etouaires, the Kuruksay p3 differs in being slightly reduced: the crown is shorter, the mesial accessory cuspid and anterior cingulum are smaller, and the p3-p4 diastema is longer. Compared to *M. megantereon* and its subspecies, the new material from Longdan exhibits a further decrease in the proportion of premolar length relative to the total tooth row length, with p3 being notably shortened in particular. Furthermore, the mesial cingulid is completely absent, and the distal cingulid is also notably reduced. Additionally, the m1 length in the Longdan new material shows a slight increase.

Megantereon adroveri and *M. whitei* are derived *Megantereon* species from Europe and Africa, respectively, and they are geologically younger than the Longdan material. The body size of the new Longdan material is comparable to, though slightly smaller than, theirs. As observed in *M. adroveri* and *M. whitei*, the upper portion of the mandibular symphysis exhibits a forward projection, a feature mentioned earlier that is particularly pronounced in *M. nihowanensis*. The degree of this projection follows the order: *M. adroveri* > *M. whitei* > new Longdan material. The type specimen of *Megantereon adroveri* originates from Venta Micena (1.6–1.5 Ma) (Pons Moyà 1987; Rodríguez-Gómez et al. 2017). Subsequently, this species was synonymized with *M. whitei* (Martínez-Navarro and Palmqvist 1995; Palmqvist et al. 2007), until Lavrov et al. (2022) reinstated the validity of *M. adroveri*. The p3 is not highly reduced in early forms of this species, whereas in late forms (e.g., Greece, APL-12) it is highly reduced. Although the p3 differs significantly between the two forms, both possess a single root and a relatively large p3-p4 diastema, albeit with the diastema being even larger in the late forms. Compared to *M. adroveri*, the new Longdan material has a shorter c-p3 diastema. Regarding the cheek teeth, the p3 size of the new Longdan material is intermediate between the early and late forms of *M. adroveri*. However, the new material possesses a longer p4 and a shorter m1. Overall, the ratio of premolar length to molar length in the new Longdan material is higher than that in *M. adroveri*. *Megantereon whitei*, established by Broom (1937), is a species characterized by an extremely reduced p3. This tooth is single-rooted and almost exclusively preserves the main cusp, with the distal accessory cuspid reduced to the distal cingulid, and there is a remarkably long diastema between p3 and p4. A specimen from Koobi Fora (KNM-ER 793B, 1.87–1.38 Ma) represents a relatively complete mandible of *M. whitei* (Werdelin and Lewis 2013). Compared to this Koobi Fora material, the new Longdan specimen exhibits a shorter c-p3 diastema, a more developed coronoid process, and greater lengths in both p4 and m1.

Megantereon is also present in the Late Early Pleistocene of Sangiran, Java, which was referred to *Megantereon* sp. by Jiangzuo et al. (2025). However, the mandibular portion of this material preserves only a single m1, and the m1 of the new Longdan material is longer than that of the Javan specimen. Moreover, in the new Longdan material, the paraconid accounts for a greater proportion of the total m1 length, and the paraconid and protoconid are more tightly connected.

Compared with the type specimen of M. microta (Fig. 4-a, b; Fig. 5)

The new Longdan material is slightly longer than the type specimen from Yanliang Cave, but distinctly more robust. We uniformly measured and numerically compared the mandibular ramus thickness below p4, with the results showing the following order: new Longdan material > *M. nihowanensis* (Nihewan, THP 00175) > *M. megantereon vakshhensis* > *M. microta* (Yanliang Cave, IVPP V19015.1). However, the new Longdan material shows increased robustness not only in the mandibular structure, but also in its incisors, canines, and cheek teeth. Furthermore, compared to the Yanliang Cave material, the new Longdan specimen possesses more developed canines, a mandibular flange, and a coronoid process. Apart from these features, however, the morphological characteristics and evolutionary grade of the new Longdan material are comparable to those of the Yanliang Cave specimen.

Morphometric analysis

To intuitively assess disparities in c-p3 diastema length, we compiled 19 samples from *M. megantereon* (n = 3, including subspecies), *M. nihowanensis* (n = 10), *M. cultridens* (n = 4), the *M. microta* holotype, and the new Longdan specimens, presenting the data as box plots. Due to missing measurements in some specimens, we utilized the ratio of the c-p3 diastema to the p3-m1 length derived from photographs, acknowledging potential bias from interspecific variation in p3-m1 length. As shown in Fig. 6, M. *megantereon* is characterized by a short c-

p3 diastema, while *M. nihowanensis* and *M. cultridens* display longer diastemas. The *M. microta* type specimen and the new Longdan material exhibit intermediate values.

To determine whether the differences between the new Longdan material and the Yanliang Cave specimen result from intraspecific variation driven by sexual dimorphism, geographical variation, or an interaction of both, we intend to conduct a cluster analysis using Principal Component Analysis (PCA). The sampled material comprises both extant and fossil specimens. The extant sample includes two large felid species, *Panthera tigris* and *Panthera pardus*, both of which exhibit pronounced sexual dimorphism. These extant specimens originate from multiple regions and have known sexes. The fossil sample consists of the *M. microta* type specimen from Yanliang Cave (IVPP V19015.1), the new Longdan material (IVPP V34763), *M. nihowanensis* (including the holotype from Nihewan, though mostly from Longdan), *M. megantereon* (QSV 146 and CECC 20161893 from Saint-Vallier, as well as the subspecies *M. megantereon vakshhensis* (No. 1-694/H), and *M. adroveri* from Dmanisi (D. 1340). A total of 17 measurements, as illustrated in Fig. 2.

The PCA results (Fig. 7) reveal significant differences between male and female individuals within each species. A slight overlap occurs, however, between some male *Panthera pardus* and female *Panthera tigris* specimens. This is attributed to total mandibular length contributing the most to Principal Component 1 (PC1), indicating that exceptionally large male leopards may exceed smaller female tigers in mandibular length. We can observe that the new Longdan specimen clusters closely with *M. microta*, but is distinctly separated from *M. nihowanensis* and *M. megantereon*. Therefore, it can be determined that the new specimen should be assigned to *M. microta*.

Interestingly, Fig. 7 places *M. megantereon vakshhensis* somewhere between the *M. megantereon* and *M. microta* clusters. We see two possible reasons for this. First, the measurements we used come from Scharapov (1986), and they cover only half of the variables, which could skew the result. Second, *M. megantereon vakshhensis* may represent a transitional form between the two species, suggesting they belong to the same evolutionary lineage.

Discussion and Conclusions

Although we assign the new Longdan material to *M. microta* based on morphological comparisons and PCA analyses, the difference in robustness between this specimen and the type specimen from Yanliang Cave in Chongzuo remains difficult to explain within the same species of *Megantereon*. Published samples of other *Megantereon* species show no clear morphological differences attributable to sexual dimorphism (Palmqvist et al. 2007) or geographic variation. Notably, *M. nihowanensis* from Chongzuo (Sabretooth Cave) shows no obvious differences from the northern specimens at Longdan and Nihewan (Zhu et al. 2020).

Generally, geographic isolation and sexual dimorphism are the two primary factors contributing to morphological variations within a species. However, neither seems to adequately explain the phenomenon observed here. Geographically, *Megantereon* exhibits notable ecological plasticity. As mentioned above, *M. nihowanensis* from the southern region shows no significant morphological divergence from northern region. This suggests that the vast geographic distance between Longdan and Chongzuo is unlikely to be the direct driver of the robustness difference in *M. microta*. Regarding sexual dimorphism, while it is common in felids, it typically manifests as a difference in overall size rather than a dramatic shift in robustness. If such extreme sexual dimorphism existed in *M. microta*, we would reasonably expect to observe similar patterns in other well-sampled *Megantereon* species, which is not the case.

As members of the subfamily Machairodontinae, mandibles of *Homotherium latidens* from the chronologically homogeneous Incarcal locality (Spain) exhibit substantial variation in ramus height, symphyseal and mental flange morphology, coronoid and angular process shape, p3 development, and overall mandibular robustness (Antón et al. 2014). Such variation is interpreted as a combined effect of ontogenetic, individual, and sexual factors. By analogy, a similar suite of intraspecific factors might underlie most of the morphological distinction between the new Longdan specimen and the *M. microta* holotype from Chongzuo.

Consequently, the most plausible explanation for the disparity is pronounced intraspecific variation coupled with our currently limited sampling of *M. microta*. The diagnostic criteria and morphological range of *M. microta* are primarily constrained by the single type specimen from Yanliang Cave. Until more complete fossil materials from different localities are discovered, this observed robustness difference should be cautiously interpreted as intraspecific variation in the species, rather than grounds for erecting a new taxon.

The presence of *M. microta* in the Longdan Fauna also provides important information for the paleoenvironment of the Linxia Basin in the Early Pleistocene. Driven by the coupled effects of Earth's orbital variations and the expansion of Northern Hemisphere ice sheets, global climate became progressively colder and drier during the Pliocene–Pleistocene transition (Hays et al. 1976; Lisiecki and Raymo 2005; Raymo et al. 2006; Hua et al. 2025). Located in the continental interior of the mid-latitudes, the Linxia Basin lies at the intersection of the Tibetan Plateau, and the Loess Plateau, occupying a unique geographic position: it straddles the boundary between the Palearctic and Oriental zoogeographic realms in China. This location places the basin like an "ecological balance" spanning the global cold-dry airflow

corridor, situated at the fragile interface of multiple climate systems, making it a classic climate-sensitive region (An et al. 2001; Deng et al. 2013).Vegetation, as the most direct responder to climatic changes in terrestrial ecosystems, underwent a gradual transition from forests to grasslands, with a major shift occurring around ~ 2.6 Ma (Hua et al. 2025). Through trophic cascades, vegetation changes directly influence herbivores and the carnivores at higher trophic levels, thereby driving faunal turnover. Conversely, changes in species composition and abundance within animal communities can serve as integrated bioindicators of historical and contemporary environmental and climatic conditions (Bai et al. 2025). Compared with contemporaneous localities, the mammalian taxa from the Longdan fauna demonstrate a distinct characteristic of body size increase. This is especially evident in canids and cervids, as well as in equids, which include very large *Equus* forms. Notably, *Coelodonta nihowanensis* displays distinct morphological adaptations to arid and cold climatic conditions, leading earlier studies to interpret the Longdan region as representing a cold, dry winter monsoon environment (Deng 2006, 2008; Biasatti et al. 2018). However, the recovery of further fossils has revealed an unusual faunal taxon, including *Ursus primitinus, Prionailurus* sp., *Hesperotherium* sp., *Manis* sp., *Postschizotherium* cf. *Intermedium* (Qiu et al. 2004; Jiangzuo et al. 2023; Xing et al. 2025). The Longdan specimens were initially assigned to Ursus yinanensis by (Qiu et al. 2009) based on worn teeth, but subsequently revised as Ursus primitinus by (Jiangzuo et al. 2023) with new material. This species represents an early-diverging lineage of the black bear group, widely distributed in southern China (Pei 1987; Liu and Qiu 2009). As a browser dependent on forested environments, *Hesperotherium* was mainly distributed in southern China and some relatively humid areas in eastern northern China (Qiu 2002; Tong 2006; Hu et al. 2025). Additionally, the morphology of *Postschizotherium* cf. *intermedium* suggests that it may have been semi-aquatic, relying on water-dependent environments (Xing et al. 2025). All of the aforementioned taxa are widely distributed throughout the warmer and humid Oriental region. Stable isotope analysis of Equidae teeth from the Longdan fauna reveals that the dominant taxon was *E. eisenmannae*, which employed an opportunistic foraging strategy, in contrast to the strong grazing preference exhibited by *Proboscidipparion sinense* (Ma et al. 2023). Collectively, this evidence suggests that the Longdan region during the Early Pleistocene was not an extremely open environment but rather a relatively humid, mosaic environments (Xing et al. 2025).

The discovery of *Megantereon microta* at the Longdan locality provides the most complete mandibular material of this species aside from the holotype from Yanliang Cave, Chongzuo, offering key insights into the morphology of its northern populations. Furthermore, this new occurrence extends the known geographic range of the species substantially northward. This finding provides new evidence that the Longdan area served as an ecotone where northern and southern Chinese faunas intermingled during the Early Pleistocene.

Declarations

Acknowledgements The authors are grateful to X. Zhu and Y. Yang for their help in accessing IOZ extant mammal collection; J. Chen and H. Si for accessing the IVPP fossil mammal collection; D. Li for accessing the IVPP extant mammal collection; R. Yang for accessing the HMV fossil mammal collection. C. Argot and G. Billet for accessing the MNHN fossil collection; B. Didier for help accessing the CCEC fossil mammal collection.

Author contributions Conceptualization of the study: Dingge Guo, Qigao Jiangzuo, Shiqi Wang, Luda Xing and Joan Madurell-Malapeira. Methodology: Qigao Jiangzuo, Joan Madurell-Malapeira and Dmitriy O. Gimranov. Formal analysis and investigation: Dingge Guo, Qigao Jiangzuo, Shiqi Wang, Peiran Li and Dongting Huang. Writing of first draft of manuscript: Dingge Guo. Writing-review and editing: Qigao Jiangzuo. Funding acquisition: Shiqi Wang and Qigao Jiangzuo. Resources: Joan Madurell-Malapeira, Dmitriy O. Gimranov, Haiyan Ma, Yi Jia and Lu Zhang. Supervision: Qigao Jiangzuo. All authors commented on previous versions of the manuscript and read and approved the final manuscript.

Funding This work was supported by National Key Research and Development Program of China 2023YFF0804501 (SW), National Natural Science Foundation of China 42572007, 42102001 (QJ) and 42430207 (TD).

Data availability All data generated or analyzed during this study are included in this published article and its supplementary information files.

Competing interests The authors declare no competing interests.

References

1. An Z, Kutzbach JE, Prell WL, Porter SC (2001) Evolution of Asian monsoons and phased uplift of the Himalaya–Tibetan plateau since Late Miocene times. Nature 411:62–66
2. Antón M, Salesa M, Galobart A, Tseng Z (2014) The Plio-Pleistocene scimitar-toothed felid genus *Homotherium* Fabrini, 1890 (Machairodontinae, Homotherini): diversity, palaeogeography and taxonomic implications. Quat Sci Rev 96:259–268

3. Bai W, Dong W, Zhang L-m, Liu W-H (2025) The Pleistocene mammalian forest dwellers in monsoon dominated provinces of China as forest dynamics proxies. Vertebr PalAsiat 63:133
4. Biasatti D, Wang Y, Deng T (2018) Paleoecology of Cenozoic rhinos from northwest China: a stable isotope perspective. Vertebr PalAsiat 56:45
5. Bravard MA (1828) Monographie de la Montagne de Perrier, près d'Issoire (Puy-de-Dôme) et de deux espèces fossiles du genre Felis, découvertes dans l'une de ses couches d'alluvion: avec une carte et deux planches. Dufour, Paris
6. Broom R (1937) On some new Pleistocene mammals from limestone caves of the Transvaal. S Afr J Sci 33:750–768
7. Deng T (2002) The earliest known wooly rhino discovered in the Linxia Basin, Gansu Province, China. Geol Bull China 21:604–608
8. Deng T (2004) Evolution of the Late Cenozoic mammalian faunas in the Linxia Basin and its background relevant to the uplift of the Qinghai-Xizang Plateau. Quat Sci 24:413–420
9. Deng T (2006) Neogene rhinoceroses of the Linxia basin (Gansu, China). In: Late Neogene and Quaternary Biodiversity and Evolution: Regional Developments and Interregional Correlations (Proceedings of the 18th International Senckenberg Conference, Volume I), pp 43–56
10. Deng T (2008) Comparison between woolly rhino forelimbs from Longdan, Northwestern China and Tologoi, Transbaikalian region. Quat Int 179:196–207
11. Deng T, Lu X, Sun D, Li S (2023) Rhinocerotoid fossils of the Linxia Basin in northwestern China as late Cenozoic biostratigraphic markers. Palaeogeogr Palaeoclimatol Palaeoecol 614:111427
12. Deng T, Qiu Z, Wang B, Wang X, Hou S (2013) Late Cenozoic Biostratigraphy of the Linxia Basin, Northweistern China. In: Wang XM, Flynn LJ, Fortelius M (eds) Fossil Mammals of Asia: Neogene Biostratigraphy and Chronology. Columbia University Press, New York, pp 243–273
13. Fang X, Li J, Zhu J, Chen H, Cao J (1997) Absolute age determination and division of the Cenozoic stratigraphy in the Linxia Basin, Gansu Province, China. Chin Sci Bull 42:1457–1471
14. Farjand A, Zhang Z, Kaakinen A, Bi S, Gibbard PL, Lihua W (2023) Rediscovery and stratigraphic calibration of the classic Nihewan Fauna, Hebei Province, China. Quat Int 646:1–10
15. Guo D, Madurell–Malapeira J, Xie K, Li Z, Qin C, Li L, Jiangzuo Q, Wang S (2025) New skull of *Megantereon inexpectatus* (Carnivora: Machairodontinae) and its implications on evolution of *Megantereon* in North China. Swiss J Palaeontol 144:73
16. Hays JD, Imbrie J, Shackleton NJ (1976) Variations in the Earth's Orbit: Pacemaker of the Ice Ages: For 500,000 years, major climatic changes have followed variations in obliquity and precession. Science 194:1121–1132
17. Hilgen FJ, Lourens LJ, Van Dam JA (2012) The Neogene Period. In: Gradstein FM, Ogg JG, Schmitz MD, Ogg GM (eds) The Geologic Time Scale. Elsevier, Amsterdam, pp 923–978
18. Hu H, Tong H, Han F, Dai H, Huang W, Jiangzuo Q, Rummy P, Wang X, Lin Y, Wei G (2025) Chronological and palaeoecological insights into the Dayakou fauna in Yanjinggou, Chongqing, China: Responses of large mammals to the Early-Middle Pleistocene Climate Transition. Quat Sci Rev 352:109199
19. Hua J, Ma J, Zhou X, Yang J, Wang S, Xiao G, Zhao K, Wang J, Hu Y, Zheng Y (2025) Climate reconstruction and mammalian faunal turnover in northern China since the late Pliocene. Palaeogeogr Palaeoclimatol Palaeoecol 680:113320
20. Jiangzuo Q, Liu J (2020) First record of the Eurasian jaguar in southern Asia and a review of dental differences between pantherine cats. J Quat Sci 35:817–830
21. Jiangzuo Q, Wang S, Deng T (2023) Chronological framework and palaeoecology of Carnivora from the Linxia Basin, China. Palaeogeogr Palaeoclimatol Palaeoecol 615:111463
22. Jiangzuo Q, Li L, Madurell-Malapeira J, Wang S, Li S, Fu J, Chen S (2022) The diversification of the lynx lineage during the Plio-Pleistocene—evidence from a new small *Lynx* from Longdan, Gansu Province, China. Biol J Linn Soc 136:536–551
23. Jiangzuo Q, van der Geer A, Volmer R, Hertler C, Li S, Guo D, Wang S, Deng T (2025) A dwarf *Megantereon* from the Sangiran complex of Java (Indonesia; late Early Pleistocene) and its biogeographic implications. J Mammal Evol 32:29
24. Lavrov A, Gimranov D, Madurell-Malapeira J, Lopatin A (2022) *Megantereon adroveri* from the Early Pleistocene of Taurida Cave, Crimea, and the European lineage of dirk-toothed cats. J Mammal Evol 29:43–49
25. Lisiecki LE, Raymo ME (2005) A Pliocene-Pleistocene stack of 57 globally distributed benthic δ18O records. Paleoceanography 20: PA1003
26. Liu JY, Qiu ZX (2009) Carnivora. In: Jin CZ, Liu JY (eds) Paleolithic Site-the Renzidong Cave, Fanchang, Anhui Province. Science Press, Beijing, pp 220–282

27. Liu P, Zhang S, Han J, Liu T (2008) Paleomagnetic chronology of Quaternary stratigraphy of the Longdan section in Gansu Province of China. Quat Sci 28:796–805
28. Liu P, Deng C, Li S, Cai S, Yuan B, Wei Q, Zhu R (2012) Magnetstratigraphic dating of the Xiashagou fauna and implication for sequencing the mammalian faunas in the Nihewan Basin, North China. Palaeogeogr Palaeoclimatol Palaeoecol 315–316:75–85
29. Liu P, Wu Z, Deng C, Tong H, Qin H, Li S, Yuan B, Zhu R (2016) Magnetostratigraphic dating of the Shanshenmiaozui mammalian fauna in the Nihewan Basin, North China. Quat Int 400:202–211
30. Liu Y, Sun L, Xu S, Ma Y, Liu P, Wang S, Luo W (2023) Cosmogenic nuclide chronological constraints on the late Cenozoic strata of the Linxia Basin, northeast Tibetan Plateau. Palaeogeogr Palaeoclimatol Palaeoecol 626:111695
31. Ma J, Sun B, Bocherens H, Deng T (2023) Dietary niche reconstruction of Pliocene and Pleistocene Equidae from the Linxia Basin of northwestern China based on stable isotope analysis. Palaeogeogr Palaeoclimatol Palaeoecol 614:111416
32. Martínez-Navarro B, Palmqvist P (1995) Presence of the African machairodont *Megantereon whitei* (Broom, 1937)(Felidae, Carnivora, Mammalia) in the Lower Pleistocene site of Venta Micena (Orce, Granada, Spain), with some considerations on the origin, evolution and dispersal of the genus. J Archaeol Sci 22:569–582
33. Nomade S, Pastre J, Guillou H, Faure M, Guérin C, Delson E, Debard E, Voinchet P, Messager E (2014) $^{40}Ar/^{39}Ar$ constraints on some French landmark Late Pliocene to Early Pleistocene large mammalian paleofaunas: Paleoenvironmental and paleoecological implications. Quat Geochronol 21:2–15
34. Palmqvist P, Torregrosa V, Pérez-Claros JA, Martínez-Navarro B, Turner A (2007) A re-evaluation of the diversity of *Megantereon* (Mammalia, Carnivora, Machairodontinae) and the problem of species identification in extinct carnivores. J Vertebr Paleontol 27:160–175
35. Pei WC (1987) Carnivora, Proboscidea and Rodentia from Liucheng Gigantopithecus cave and other caves in Guangxi. Mem Inst Vertebr Palaeontol Palaeoanthropol Acad Sin 18:1–119
36. Pons Moyà J (1987) Los carnivoros, Mammalia de Venta Micena, Granada, España. Paleontol Evol Mem Espec 1:109–128
37. Qiu Z (2000) Nihewan fauna and Q/N boundary in China. Quat Sci 20:142–154
38. Qiu Z (2002) *Hesperotherium*-A new genus of the last chalicotheres. Vertebr PalAsiat 40:317
39. Qiu Z, Deng T, Wang B (2004) Early Pleistocene mammalian fauna from Longdan, Dongxiang, Gansu, China. Science Press, Beijing
40. Qiu Z, Deng T, Wang B (2009) First bear material from Dongxiang, Gansu—Addition to the longdan mammalian fauna (2). Vertebr PalAsiat 47:245
41. Qiu Z, Deng T, Wang B (2014) A Late Miocene *Ursavus* skull from Guanghe, Gansu, China. Vertebr PalAsiat 52:265
42. Raymo ME, Lisiecki L, Nisancioglu KH (2006) Plio-Pleistocene ice volume, Antarctic climate, and the global $\delta^{18}O$ record. Science 313:492–495
43. Rodríguez-Gómez G, Palmqvist P, Ros-Montoya S, Espigares MP, Martinez-Navarro B (2017) Resource availability and competition intensity in the carnivore guild of the Early Pleistocene site of Venta Micena (Orce, Baza Basin, SE Spain). Quat Sci Rev 164:154–167
44. Scharapov S (1986) The Kuruksay Complex of Upper Pliocene Mammalian of Afghan-Tadjik Depression. Donish, Dushanbe
45. Scharapov S (1996) Säbelzahnkatzen (Mammalia: Carnivora: Machairodontinae) aus dem späten Känozoikum Tadschikistans. Senckenb Lethaea 76:251–257
46. Shi QQ (2023) Fossil bovids from the Linxia Basin of Gansu Province, China, and their implications for regional biostratigraphy, palaeogeography and palaeoecology. Palaeogeogr Palaeoclimatol Palaeoecol 619:111543
47. Tong H (2006) Hesperotherium sinense, a chalicothere (Perissodactyla, Mammalia) from the Early Pleistocene Liucheng Gigantopithecus Cave. Vertebr PalAsiat 44:347
48. Wang X, Flynn LJ, Deng C (2023) A review of the Cenozoic biostratigraphy, geochronology, and vertebrate paleontology of the Linxia Basin, China, and its implications for the tectonic and environmental evolution of the northeastern margin of the Tibetan Plateau. Palaeogeogr Palaeoclimatol Palaeoecol 628:111775
49. Werdelin L, Lewis ME (2013) Koobi Fora Research Project, Volume 7: The Carnivora. California Academy of Sciences, San Francisco
50. Xing LD, Wang XB, Pickford M, Chen YJ, Ma J, Wang SQ, Liu YY, Wang SQ (2025) The first cranium of *Postschizotherium* (Pliohyracidae, Hyracoidea) from the Lower Pleistocene of China. Palaeoworld 35(1):200998
51. Xue X, Zhang Y, Yue L (2006) Paleoenvironments indicated by the fossil mammalian assemblages from red clay-loess sequence in the Chinese Loess Plateau since 8.0 Ma BP. Sci China Ser D 49:518–530
52. You Y, Liu H, Pan Y (1978) Plio-Pleistocene deposits and mammalian faunas of Yuanmou Basin, Yunnan. Prof Pap Stratigr Palaeontol 7:40–67

53. Zan J, Fang X, Zhang W, Yan M, Zhang T (2016) Palaeoenvironmental and chronological constraints on the Early Pleistocene mammal fauna from loess deposits in the Linxia Basin, NE Tibetan Plateau. Quat Sci Rev 148:234–242
54. Zhang Z, Feng X (2004) Mammalia. In: Zheng SH (ed) Jianshi Hominid Site. Science Press, Beijing, pp 67–303
55. Zhu M, Schubert BW, Liu J, Wallace SC (2014) A new record of the saber-toothed cat *Megantereon* (Felidae, Machairodontinae) from an early Pleistocene Gigantopithecus fauna, Yanliang cave, Fusui, Guangxi, South China. Quat Int 354:100–109
56. Zhu M, Jiangzuo Q, Qin D, Jin C, Sun C, Wang Y, Yan Y, Liu J (2020) First discovery of *Megantereon* skull from southern China. Hist Biol 33:3413–3422

Figures

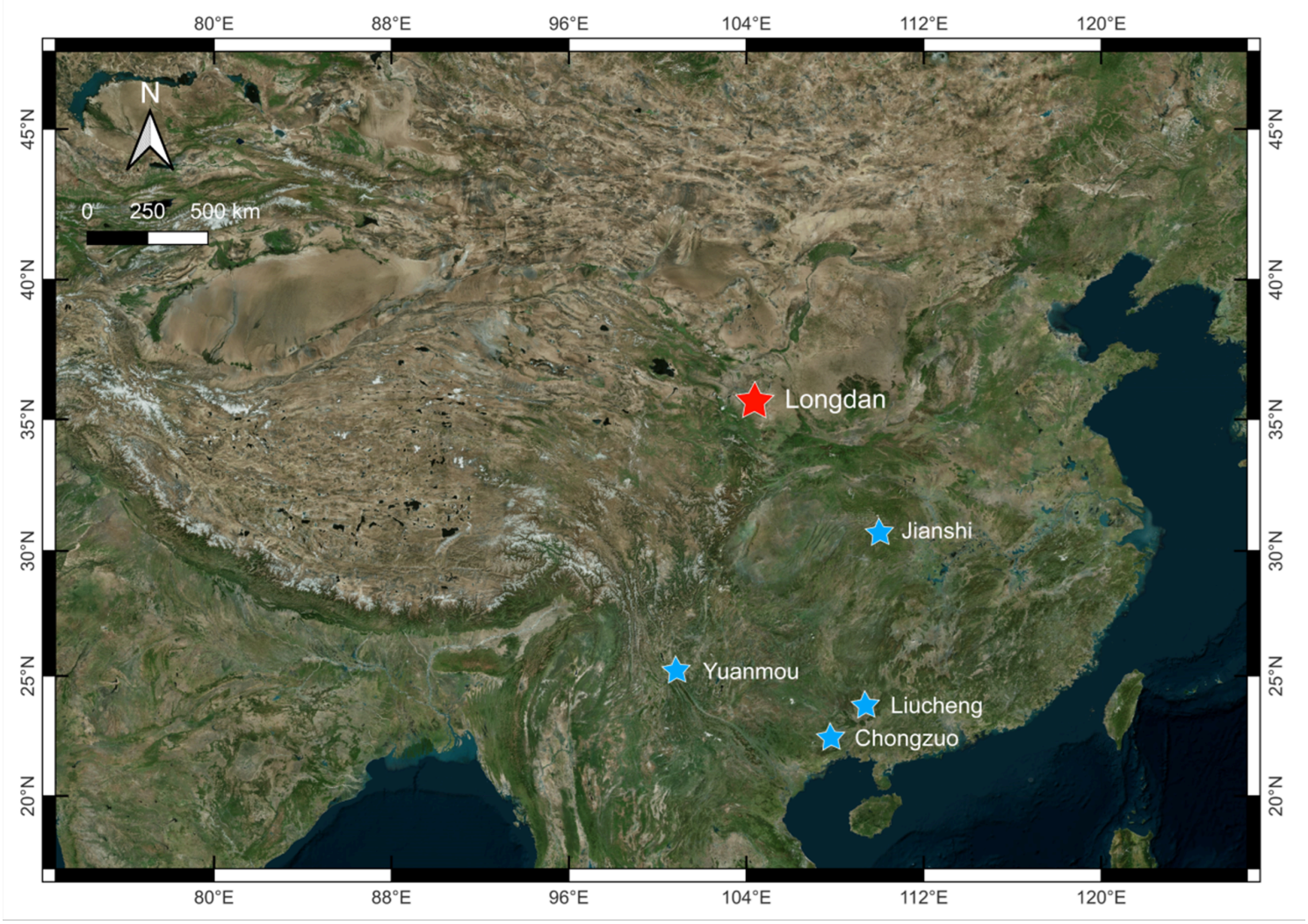


Figure 1

Fossil localities of *Megantereon microta*in China. The red star shows the locality of the new material, the blue star shows the other locality of *M. microta*

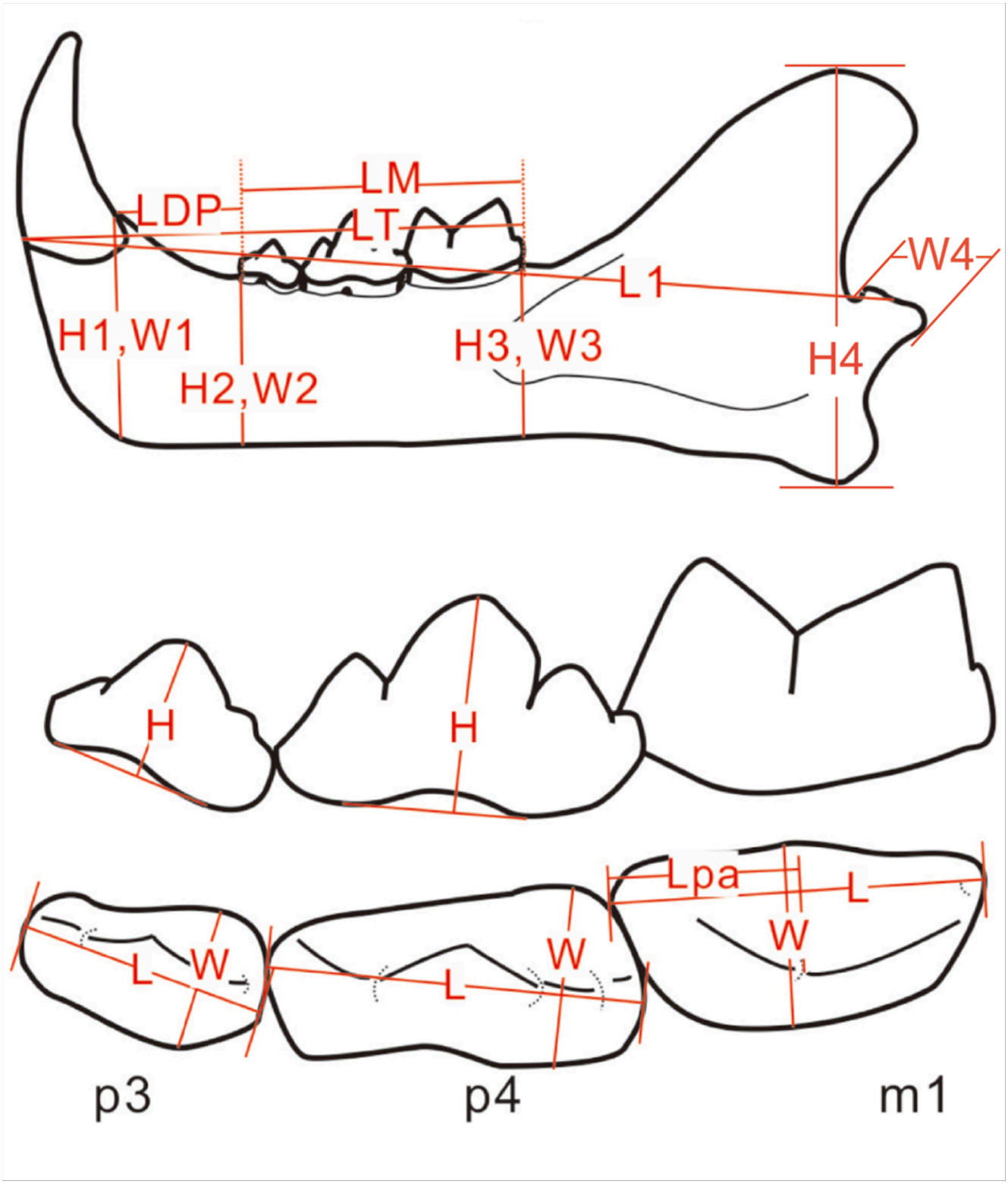


Figure 2

Mandibular and dental measurements for felids. **H1-3** and **W1-3**in the mandible represent the mandibular height and width posterior to the canine, anterior to the p3, and posterior to the m1.

H4represents the maximum vertical height from the apex of the coronoid process to the base of the angular process. **W4** represents the maximum mediolateral transverse width of the condylar process

Anatomical abbreviations

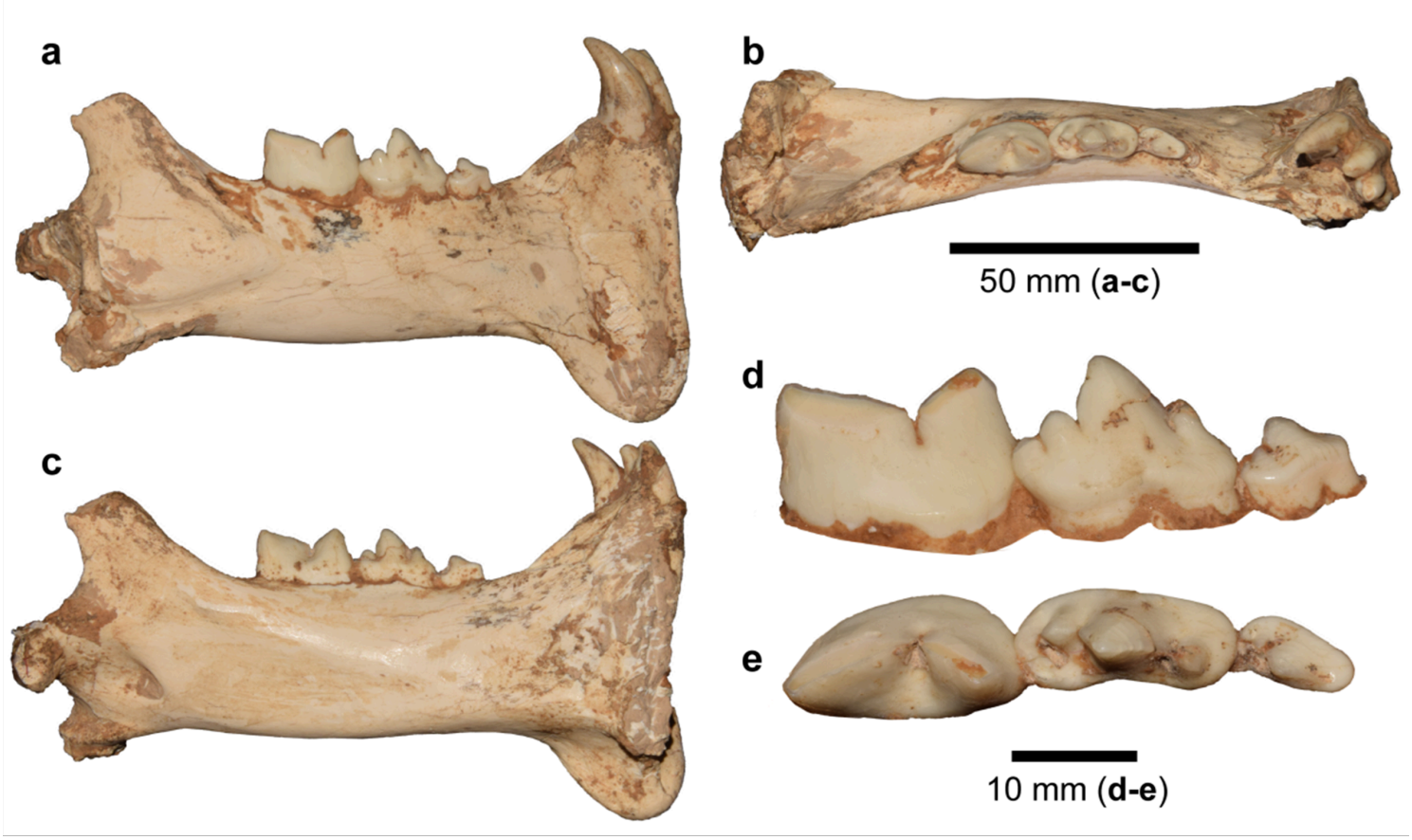


Figure 3

Megantereon microta mandible with i2-c1 and p3-m1 from Longdan (IVPP V34763) in buccal (**a**), occlusal (**b**), and lingual (**c**) view; detail of p3-m1 in buccal (**d**), and occlusal (**e**) view. Scale bars equal 5 cm in **a-c**, and 1 cm in **d-e**

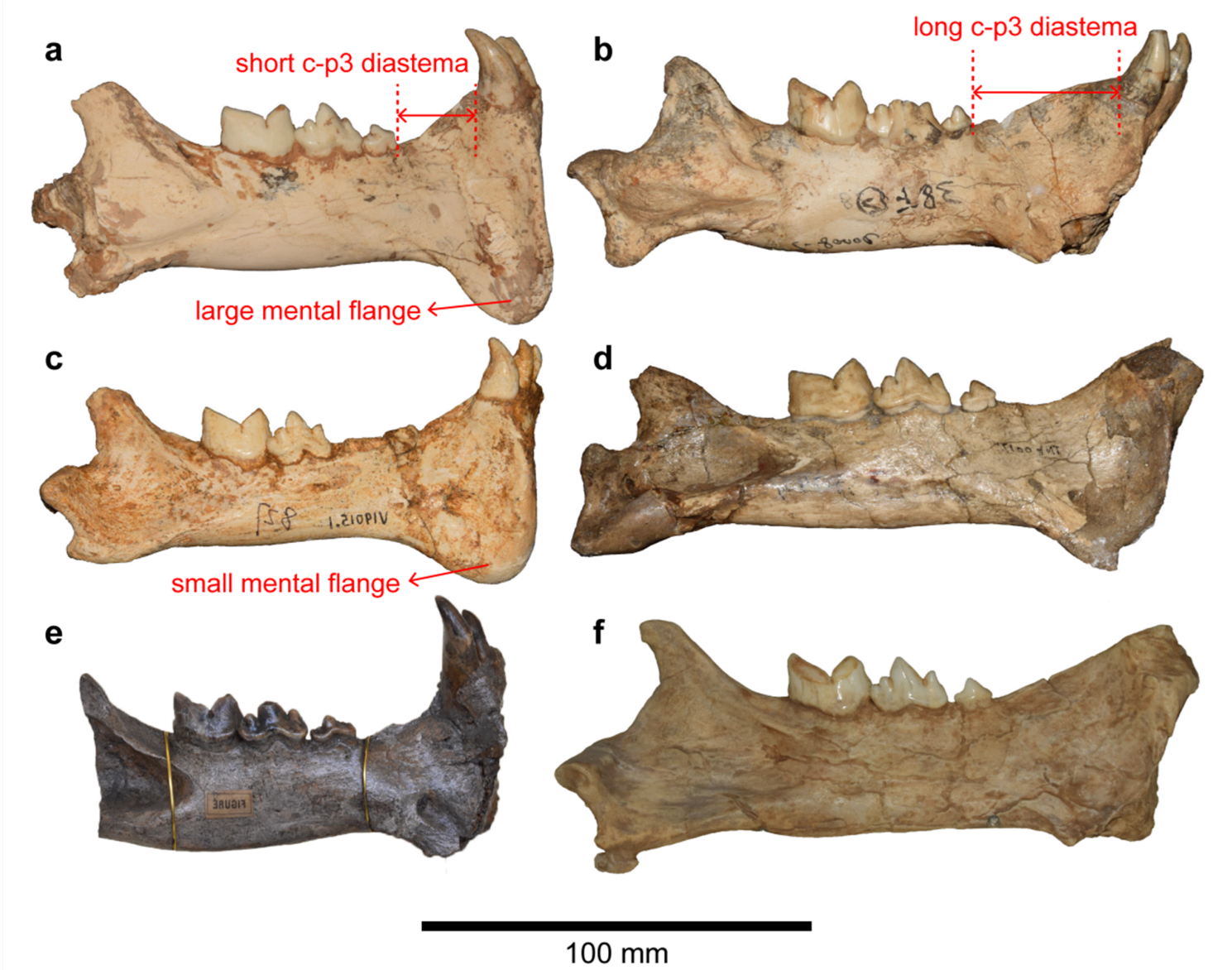


Figure 4

Comparison of the mandible of *Megantereon*. **a**. *Megantereon microta* (IVPP V34763, Longdan); **b**. *M. nihowanensis* (HMV 1214, Longdan); **c**. *M. microta* (IVPP V19015, Yanliang Cave, Chongzuo); **d**. *M. nihowanensis* (THP 00175, Nihewan); **e**. *M. megantereon* (MNHN 1094, Les Etouaires); **f**. *M. cultridens*(FP1-2002-1391, Fonelas Pocico 1; housed in the Museo Arqueológico y Paleontológico de la Comunidad de Madrid, photographed at Dientes de Sable). Scale bar equals 10 cm

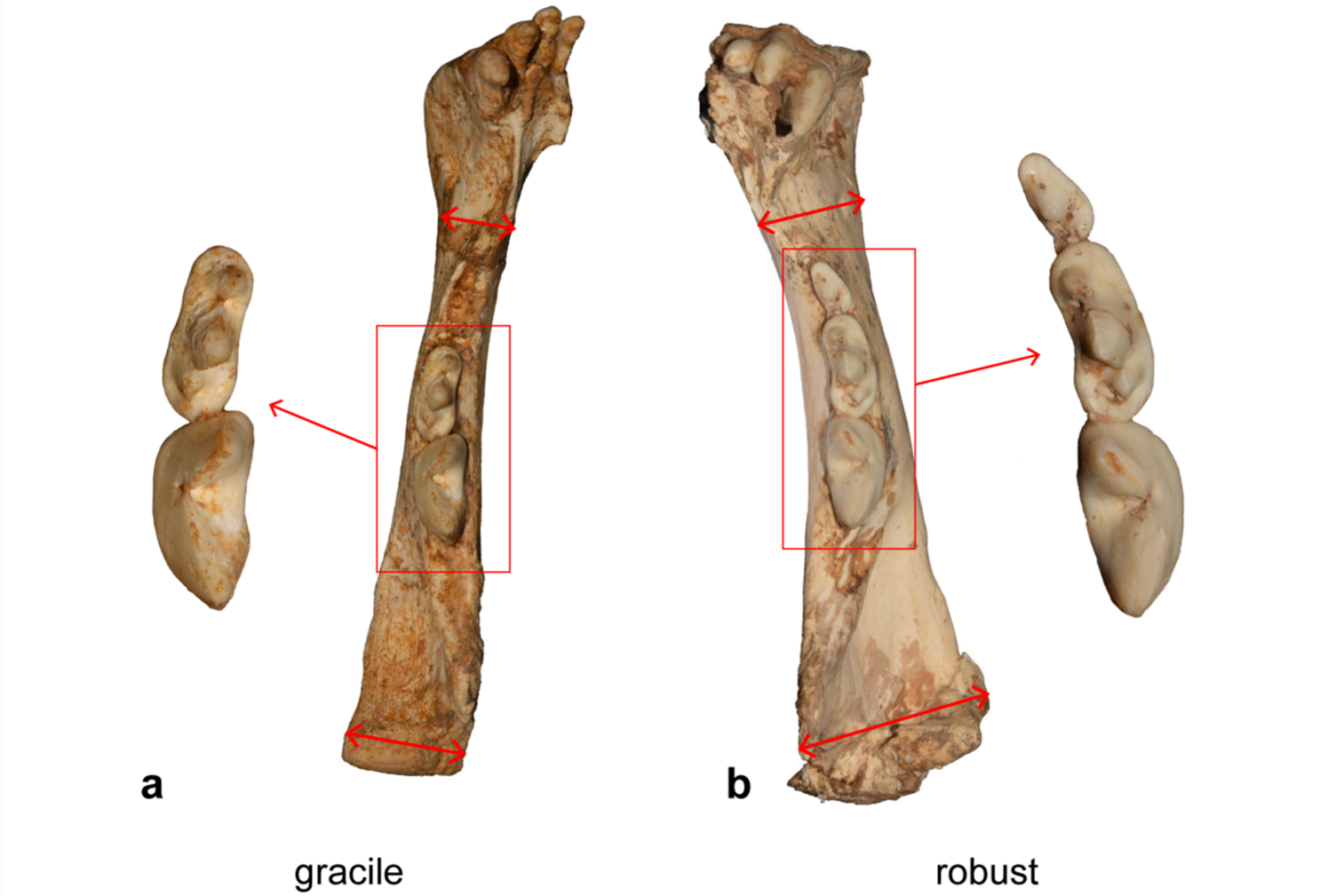


Figure 5

Comparison of *M. microta* from different localities. **a**. IVPP V19015, Chongzuo; **b**. IVPP V34763, Longdan. Not to scale

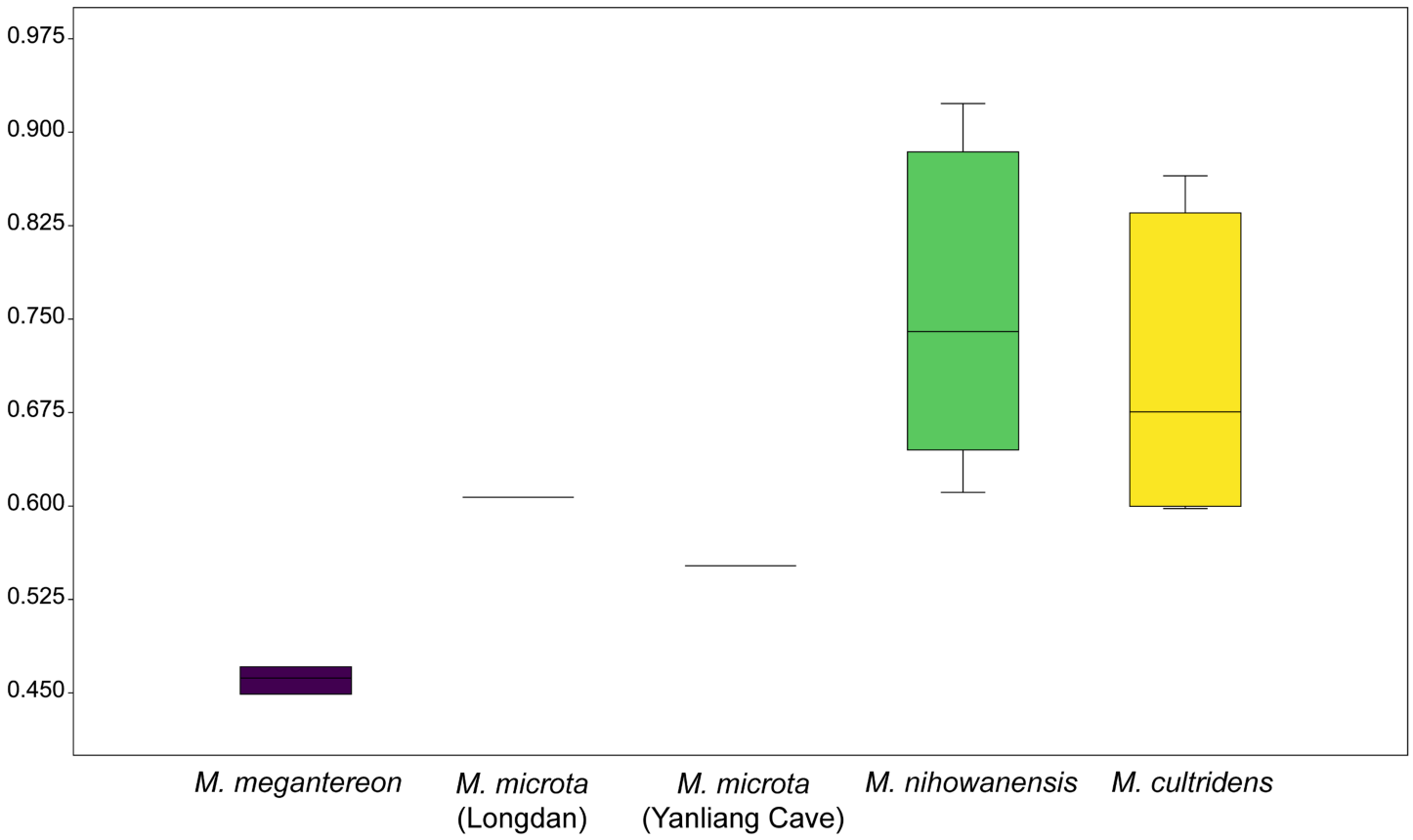


Figure 6

Box plot of the D c-p3 / p3-m1 ratio in *Megantereon*

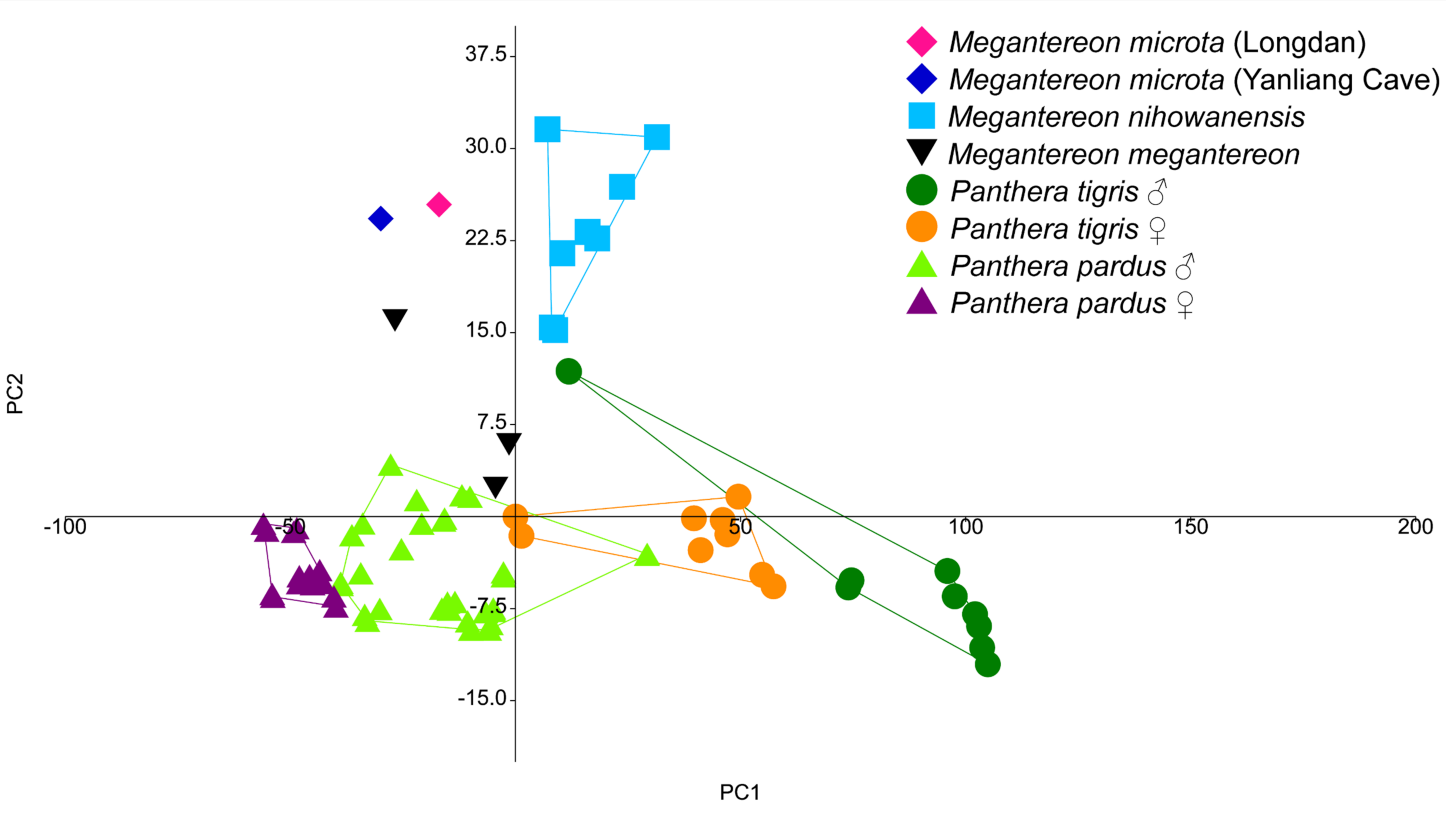


Figure 7

Principal Component Analysis (PCA) plot. The black inverted triangle, positioned further upper-left and slightly deviating from the *M. megantereon*cluster, represents its subspecies *M. megantereon vakshhensis*

Supplementary Files

This is a list of supplementary files associated with this preprint. Click to download.

- Boxplot.dat
- PCA.dat